Photoemission Electron Microscopy as a Tool for the Investigation of Optical Near Fields

M. Cinchetti, A. Gloskovskii, S. A. Nepjiko, and G. Schönhense
Johannes Gutenberg-Universität, Institut für Physik, 55099 Mainz, Germany

H. Rochholz and M. Kreiter*
Max Planck Institut für Polymerforschung, 55128 Mainz, Germany
(Received 15 December 2004; published 21 July 2005)

Photoemission electron microscopy was used to image the electrons photoemitted from specially tailored Ag nanoparticles deposited on a Si substrate (with its native oxide SiO_x). Photoemission was induced by illumination with a Hg UV lamp (photon energy cutoff $\hbar\omega_{UV} = 5.0$ eV, wavelength $\lambda_{UV} = 250$ nm) and with a Ti:sapphire femtosecond laser ($\hbar\omega_l = 3.1$ eV, $\lambda_l = 400$ nm, pulse width below 200 fs), respectively. While homogeneous photoelectron emission from the metal is observed upon illumination at energies above the silver plasmon frequency, at lower photon energies the emission is localized at tips of the structure. This is interpreted as a signature of the local electrical field therefore providing a tool to map the optical near field with the resolution of emission electron microscopy.

DOI: 10.1103/PhysRevLett.95.047601 PACS numbers: 79.60.Jv, 78.67.Bf

The intensity of optical fields may be largely enhanced in the vicinity of nanoscopically structured metal objects. Extreme local field enhancement is believed to be responsible for the increase of the Raman cross section of organic molecules by up to a factor of 10^{14} [1] in the vicinity of stochastically roughened silver films. Fluorescence as well is drastically altered by an enhanced optical near field which was shown to improve the performance of chromophores [2,3] and semiconductor quantum dots [4] significantly. These effects are in general explained in terms of an increased coupling of a local absorbing or emitting dipole with both incident and outgoing far field photons, such affecting both the optical excitation and the emission process. In analogy to antenna used for radiation of lower frequency, in this context metal objects can be regarded as antenna for the optical regime. These nanoscopic antenna are characterized by an overall optical resonance similar to the well-known plasmon resonance of spherical metal particles [5,6]. Such resonances have been observed for rods [7], closely spaced particle dimers [8] and nanorings [9], to name only a few. In all these cases a strong dependence of the resonance wavelength on the geometry was found. An important additional requirement for a good antenna is geometrical features of very small dimensions that focus the optical field to extremely high intensities in volumes far below the diffraction limit. One prominent example is the nanoscopic gap that is formed between two almost touching metal spheres [10] or cylinders [11] or between a plane and a sphere [12]. Sharp tips are another important example for nanoscale structures where it could be shown experimentally [13] that the photophysics of a single fluorescent molecule is significantly altered by the large field enhancements, this result being in qualitative agreement with theory [14].

Mapping of the near field distribution down to the nanometer scale is the key to understand and optimize such antenna structures. Fluorescence microscopy [15] has been used for the mapping of near fields, but this method is restricted to the structure of the near field above the diffraction limit. Near field optical microscopy has proven to give a resolution down to some 10 nm [16]. It must be pointed out, though, that metal tips which provide a good optical resolution form, if approaching the object under study, a highly complex metal structure which is composed of tip and sample, possessing a nanoscopic gap between tip and object. The optical response is in turn strongly altered, preventing the optical characterization of the sample object alone. Dielectric tips are less perturbing but have only a limited resolution. They have been used to investigate the optical near fields of several plasmonic nanostructures [17]. The use of almost pointlike probes for the near field such as a single molecule [18] or the end of a carbon nanotube [19] circumvents the aforementioned problems, but the experimental difficulties prevent these approaches from being applicable as a standard method for the investigation of a larger amount of samples. An approach to use the high resolution of electron microscopy was demonstrated by Yamamoto *et al.* [20] who detected light emission induced by an electron beam and were able to image multipolar patterns on small silver particles, taking advantage of the superior resolution of electron optics.

Photoelectron emission has been shown to be enhanced by the increase of the local electrical field upon excitation of the particle plasmon of small silver clusters [21]. In this context, photoemission dynamics of surface-bound silver particles was studied in detail [22] and the influence of the collective electron dynamics could be quantified [23,24] as well as charging of the particles [22]. However, in the above mentioned works the photoemission signal was recorded without lateral resolution. In this Letter it is shown that photoemission electron microscopy (PEEM) can be used to map the near field distribution. Using the same experimental technique, we have previously been able to localize regions on inhomogeneous Ag and Cu

surfaces where laser illumination excites collective electron modes or localized surface plasmons (LSP). Laterally resolved electron energy distribution spectra have shown that the LSP-induced enhanced near field affects the photoemission and its dynamics in a crucial way [25,26]. In these experiments the structural features giving rise to the locally enhanced photoemission yield were not known and remained speculative. For this reason, we present in this publication experiments on well-defined metal structures that possess sharp tips as required for high local field enhancement.

Nanoscopic crescent-shaped silver objects were prepared on a Si wafer using a combination of colloid templating, metal film deposition, and ion beam milling [27]. Figure 1 shows a typical scanning electron microscopy (SEM) image of the crescents with a diameter of roughly 400 nm and a thickness of 50 nm. Photoelectron emission was induced by illuminating the sample with two different light sources. A Hg deep-UV lamp (photon energy cutoff $\hbar\omega_{\mathrm{UV}} = 5.0$ eV, wavelength $\lambda_{\mathrm{UV}} \geq 250$ nm), was focused on the sample at an angle $\theta = 65°$ with respect to the surface normal. The fundamental of a femtosecond Ti:sapphire laser (MaiTai Spectra Physics, wavelength tunable between 750 nm and 850 nm, repetition rate 80 MHz) was frequency doubled by a commercial device (3980 Spectra Physics), giving a photon energy tunable between 2.9 and 3.3 eV and a pulse width below 200 fs. For this experiment the photon energy was kept fixed at $\hbar\omega_l = 3.1$ eV ($\lambda_l = 400$ nm). The frequency-doubled beam was focused on the sample at $\theta = 65°$, from the opposite direction in the same plane of incidence as the UV lamp. The obtained fluence per pulse was about 6.4 $\mu\mathrm{J\,cm^{-2}}$. A Fresnel rhomb allowed one to adjust the direction of the polarization vector (p polarization). The photoemission electron microscope was a commercial instrument (Focus IS-PEEM). Model calculations were performed in order to illustrate the dependence of the optical response of silver on photon energy. For the calculations, the optical response of silver was described by literature values [28] and a two-dimensional geometry of an infinitely extending rod with a cross section similar to the crescents was considered. Maxwell equations were solved with a commercial finite element code (Femlab GMBH, Göttingen).

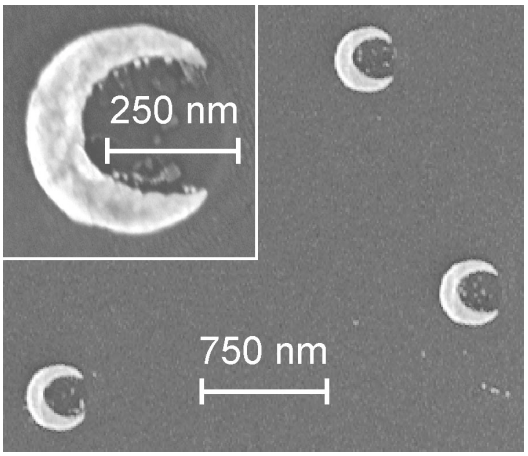

FIG. 1. Scanning electron micrograph of the silver crescents. The inset shows a magnified view.

In a PEEM image, the brightness in a given area is proportional to the intensity of electron emission from that area. Thus, for the interpretation of the data it is important to know the physical processes leading to electron emission for a certain wavelength of the incident light. The work function ϕ of Ag ranges between 4.2 and 4.8 eV [29], depending on crystal orientation. Upon illumination of the sample with the UV lamp, electrons are emitted by regular, one-photon photoemission (1PPE), since $\hbar\omega_{\mathrm{UV}} > \phi$. On the other hand, under laser illumination at $\lambda = 400$ nm $\hbar\omega_l = 3.1$ eV, the photon energy is smaller than the work function and photoemission requires a multiphoton process, where it can be expected that two-photon processes as lowest order dominate. The presence of a Fermi edge in the laterally resolved electron energy distribution spectra recorded from Cu and Ag nanoclusters [25,26] demonstrates that even in this case 2PPE gives a substantial contribution to the recorded electron yield. As a first approximation it can be assumed that in this case the electron emission yield scales with the square of near field photon density [30]. This corresponds to the fourth power of the local electric field that, especially for LSP-resonant metal particles, may significantly differ from the field of the incoming wave [24]. Because of the inelastic mean free path of the electrons, PEEM probes only the first few nm (at our energies about 5 nm) from the surface, thus giving a fingerprint of the electrical field in this region. This quantity is crucial to understand the aforementioned luminescence enhancement effects and is difficult to access by alternative near field imaging techniques. Details of the interaction of the local electric field E with the electrons

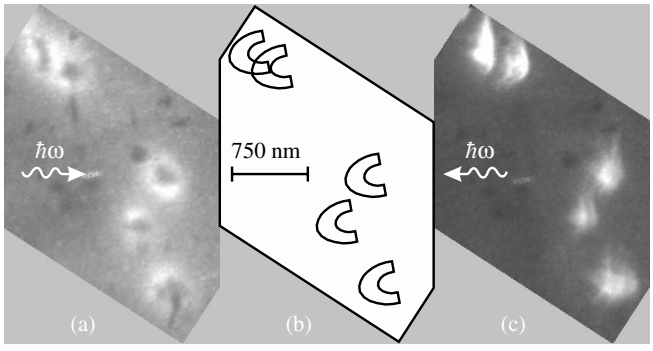

FIG. 2. High-resolution PEEM images of the same region of the sample. (a) UV-PEEM image, $\hbar\omega_{\mathrm{UV}} = 5.0$ eV (exposure time $\Delta t = 200$ s). (b) Schematic drawing to indicate the position of the silver crescents on the sample. (c) Laser-PEEM image, $\hbar\omega_l = 3.1$ eV (exposure time $\Delta t = 5$ s). The arrows indicate the direction of illumination. Both images (a) and (c) have been digitally processed to enhance the contrast.

certainly must take into account the vector character of E as well as the nature of the states from where electrons are emitted.

Figures 2(a) and 2(c) show a UV-PEEM image and a laser-PEEM image of the same region of the sample, respectively. The photoemission signal of five silver crescents is visible in both images. In particular, in 2(a) five ringlike structures can be identified. To help the eye of the reader, we added Fig. 2(b) to indicate the position and orientation of the crescents. In 2(c) the photoemission yield is enhanced in different positions than in 2(a). Note that the dark spots visible in Fig. 2(a) are due to defects on the imaging unit of the photoemission electron microscope and must not be interpreted as part of the electron emission map. Figures 3(a) and 3(b) show a magnification of the third crescent from the top in Figs. 2(a) and 2(c) for the two illumination modes. The dark spot in the upper left corner is one of the above mentioned defects. The images for UV and laser excitation reveal a marked difference. In particular, comparison to the orientation of the crescents 3(c) suggests that upon UV illumination electron emission is enhanced throughout the metal structure. Some highly localized features that are different for the individual objects are superimposed on this average behavior. Illumination at $\lambda = 400$ nm, on the other hand, leads to an enhanced emission between the tips of the structure. These observations can be explained by consideration of the dielectric response of silver [28]. At the experimentally used wavelengths silver has a dielectric function of $\epsilon(250\ \text{nm}) = -0.1377 + 3.5046\imath$ and $\epsilon(400\ \text{nm}) = -4.4604 + 0.2147\imath$. The dominating imaginary part for $\epsilon(250\ \text{nm})$ indicates that this radiation corresponds to an energy above the onset of interband transitions. The dominating negative real part of $\epsilon(400\ \text{nm})$ is typical for all energies below the interband transitions: this behavior rules the entire frequency range down to the static limit and may be termed the ''metallic'' response.

Figure 4 shows calculations for a cross section through a silver rod in vacuum to illustrate qualitatively the optical near field distribution for these two cases. At $\lambda = 250$ nm, there is an almost homogeneous field inside the silver, while at $\lambda = 400$ nm enhanced and highly localized optical fields are observed, especially near the tips. This calculation must not be regarded as a quantitative description of the electromagnetic response of the crescents since they are 50 nm thick structures on an interface between two media with highly different polarizabilities (vacuum and silicon), whereas the calculations are performed on infinitely extending rods *in vacuo*. Still, the central conclusion of a qualitatively different response of the metal objects to optical fields above and below the onset of interband transitions is justified and in agreement with theoretical studies on similar geometries [11,14].

As a general trend, it can be stated that the particle plasmon wavelength given by $\text{Re}(\epsilon) = -2$ roughly divides a regime of metallic behavior at lower photon energies where large field enhancements and optical resonances are observed from a nonmetallic regime, i.e., a response without significant change of the field distribution of the exciting photon beam at higher energies. Our experimental observations can be interpreted along these lines; homogeneous electron emission from the entire silver surface should appear as a 1:1 image of the geometrical shape of the crescents for the case of UV illumination above the particle plasmon energy. This image is expected to be smeared out due to convolution with the point spread function of the photoemission electron microscope, explaining the observation of ringlike structures in Fig. 2(a). The localized differences from ring to ring are partly due to imperfections in the crescents that may influence the electron emission process in a way independent of the optical field strength (topographic contrast). It is noted, though, that for silver particles the peculiar property of a blueshifted plasmon frequency for very small particles is observed [31], which may point towards another possible source for localized highly emissive spots at grains or cracks in the metal crescents in the UV. As a consequence of these superimposed effects, the signature of the opening of the ring, which should in principle be visible, is highly obstructed. In the laser-PEEM image [Fig. 3(b)], the enhanced 2PPE yield at the gap position points towards a locally enhanced electrical optical field

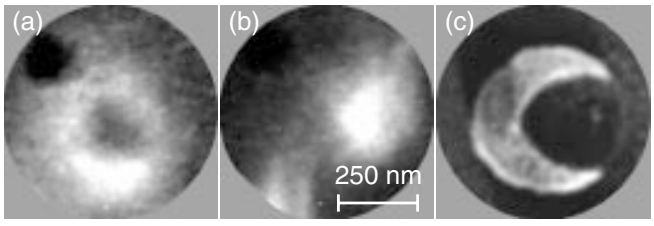

FIG. 3. (a) Magnification of the third crescent from the top in Fig. 2(a), $\hbar\omega_{\text{UV}} = 5.0$ eV. (b) Magnification of Fig. 2(c), $\hbar\omega_l = 3.1$ eV. (c) Corresponding SEM image of a crescent with identical orientation and scale.

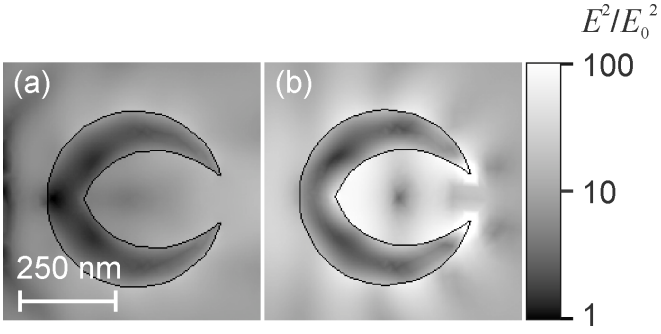

FIG. 4. Local magnitude of the electric field, calculated for a 2D geometry of silver in vacuum for light incident from the left with wavelength (a) $\lambda_{\text{UV}} = 250$ nm and (b) $\lambda_l = 400$ nm. The gray scale bar indicates the enhancement factor of the squared field amplitude.

close to the tips of the structure in agreement with the behavior that can be expected for a photon energy in the vicinity of the particle plasmon energy.

In summary, it has been shown experimentally for defined metal structures that local optical fields can be imaged directly by PEEM, a technique that can reach a lateral resolution down to 20 nm [32]. This provides an easy-to-use method for the quantitative investigation of local field distributions (E^2 or E^4) at the surface. Note that our approach provides information that is different from the light emission induced by electron beams which was reported already [20]. In such experiments photons are generated by electrons passing the optical antenna, such giving information on the 3D electrical field distribution around the antenna, similarly to scanning near field optical microscopy experiments [16–19]. The PEEM method therefore promises to shed more light on the optical near field right at the metal surface, which up to now has been very difficult to access quantitatively. It should be noted that the description of the electromagnetic response in terms of a macroscopic dielectric function $\epsilon(\omega)$ can only be regarded as a first approximation near the surface of the material from where the photoelectrons are emitted. For the metallic structure the microfields in this region are influenced by the oscillating surface charges, being located in the electron spill-out region [31]. In the gap of the crescents the photoemission signal comes from the surface region of the oxide-covered silicon. Here, the local field is modified by the properties of the vacuum-substrate interface. For both cases the near field cannot be treated properly using an ansatz for a sharp interface between vacuum and material. It will be a challenging task for the future to develop a more refined model giving a proper description of the field right at the surface. To reach this goal, we are also working on an optimized sample preparation with reduced individual differences between the objects under study. Then, more experiments in combination with reliable theoretical predictions and independent purely optical reference experiments are planned to achieve a complete understanding of the factors influencing the image formation.

We acknowledge financial support from BMBF Projects No. 03N8702 and No. 03N6500.

Note added.—A similar approach as presented here was shown recently for time-resolved imaging of surface plasmon fields on gratings [33].

*Electronic address: kreiter@mpip-mainz.mpg.de

[1] S. Nie and S. R. Emory, Science **275**, 1102 (1997).
[2] A. Wokaun, Mol. Phys. **56**, 1 (1985).
[3] J. R. Lakowicz *et al.*, J. Fluoresc. **14**, 425 (2004).
[4] K. T. Shimizu, W. K. Woo, B. R. Fisher, H. J. Eisler, and M. G. Bawendi, Phys. Rev. Lett. **89**, 117401 (2002).
[5] C. F. Bohren and D. R. Huffmann, *Absorption and Scattering of Light by Small Particles* (John Wiley, New York, 1983).
[6] U. Kreibig and M. Vollmer, *Optical Properties of Metal Clusters* (Springer-Verlag, Berlin, 1992).
[7] C. Sönnichsen, T. Franzl, T. Wilk, G. von Plessen, J. Feldmann, O. Wilson, and P. Mulvaney, Phys. Rev. Lett. **88**, 077402 (2002).
[8] T. Okamoto and I. Yamaguchi, J. Phys. Chem. B **107**, 10321 (2003).
[9] J. Aizpurua, P. Hanarp, D. S. Sutherland, M. Käll, G. W. Bryant, and F. J. Garcia de Abajo, Phys. Rev. Lett. **90**, 057401 (2003).
[10] P. K. Aravind, A. Nitzan, and H. Metiu, Surf. Sci. **110**, 189 (1981).
[11] J. P. Kottmann and O. J. F. Martin, Opt. Express **8**, 655 (2001).
[12] P. K. Aravind and H. Metiu, Surf. Sci. **124**, 506 (1983).
[13] A. Kramer, W. Trabesinger, B. Hecht, and U. P. Wild, Appl. Phys. Lett. **80**, 1652 (2002).
[14] J. P. Kottmann, O. J. F. Martin, D. R. Smith, and S. Schultz, Phys. Rev. B **64**, 235402 (2001).
[15] H. Ditlbacher, J. R. Krenn, N. Felidj, B. Lamprecht, G. Schider, A. Leitner, and F. Aussenegg, Appl. Phys. Lett. **80**, 404 (2002).
[16] H. G. Frey, F. Keilmann, A. Kriele, and R. Guckenberger, Appl. Phys. Lett. **81**, 5030 (2002).
[17] J. R. Krenn, J. C. Weeber, A. Dereux, E. Bourillot, J. P. Goudonnet, B. Schider, A. Leitner, F. R. Aussenegg, and C. Girard, Phys. Rev. B **60**, 5029 (1999).
[18] J. Michaelis, C. Hettich, J. Mlynek, and V. Sandoghdar, Nature (London) **405**, 325 (2000).
[19] R. Hillenbrand, F. Keilmann, P. Hanarp, D. S. Sutherland, and J. Aizpurua, Appl. Phys. Lett. **83**, 368 (2003).
[20] N. Yamamoto, K. Araya, and F. J. Garcia de Abajo, Phys. Rev. B **64**, 205419 (2001).
[21] J. Lehmann, M. Merschdorf, W. Pfeiffer, A. Thon, S. Voll, and G. Gerber, Phys. Rev. Lett. **85**, 2921 (2000).
[22] W. Pfeiffer, C. Kennerknecht, and M. Merschdorf, Appl. Phys. A: Mater. Sci. Process. **78**, 1011 (2004).
[23] M. Scharte, R. Porath, T. Ohms, M. Aeschlimann, J. R. Krenn, H. Ditlbacher, F. R. Aussenegg, and A. Liebsch, Appl. Phys. B **73**, 305 (2001).
[24] M. Merschdorf, C. Kennerknecht, and W. Pfeiffer, Phys. Rev. B **70**, 193401 (2004).
[25] M. Cinchetti, D. A. Valdaitsev, A. Gloskovskii, A. Oelsner, S. Nepijko, and G. Schönhense, J. Electron Spectrosc. Relat. Phenom. **137–140**, 249 (2004).
[26] M. Cinchetti and G. Schönhense, J. Phys. Condens. Matter **17**, S1319 (2005).
[27] J. Shumaker-Parry, H. Rochholz, and M. Kreiter, Adv. Mater. (to be published).
[28] P. B. Johnson and R. W. Christy, Phys. Rev. B **6**, 4370 (1972).
[29] H. B. Michaelson, J. Appl. Phys. **48**, 4729 (1977).
[30] V. M. Shalaev, C. Douketis, T. Haslett, T. Stuckless, and M. Moskovits, Phys. Rev. B **53**, 11 193 (1996).
[31] A. Liebsch, Phys. Rev. B **48**, 11 317 (1993).
[32] C. Ziethen *et al.*, J. Electron Spectrosc. Relat. Phenom. **88–91**, 983 (1998).
[33] A. Kubo, K. Onda, H. Petek, Z. Sun, Y. S. Jung, and H. K. Kim, Nano Lett. **5**, 1123 (2005).